Assessment and Modeling of a Sequential Process for Water Treatment-Adsorption and Batch CWAO Regeneration of Activated Carbon

Carine Julcour-Lebigue, Nguessan Joachim Krou, Caroline Andriantsiferana, Anne-Marie Wilhelm, Henri Delmas

ASSESSMENT AND MODELING OF A SEQUENTIAL PROCESS FOR WATER TREATMENT- ADSORPTION AND BATCH CWAO REGENERATION OF ACTIVATED CARBON

Carine Julcour-Lebigue*, Nguessan Joaquim Krou, Caroline Andriantsiferana, Anne-Marie Wilhelm†, Henri Delmas

Université de Toulouse, INP, LGC (Laboratoire de Génie Chimique),4 allée Emile Monso, BP 84234, 31432 Toulouse Cedex 4, France
CNRS, LGC, 31432 Toulouse Cedex 4, France

Abstract

A new sequential process - AD-OX - for (post)treatment of water polluted by poorly biodegradable organic compounds has been investigated. It is based on hybridizing classical adsorption on a fixed bed of activated carbon (AC) followed by batch wet catalytic oxidation at higher temperature and pressure on the same bed of AC, which is then regenerated in situ. The basic idea is to take advantage of both operations: 1-efficient water purification at room temperature by adsorption, 2-effective concentrated pollutant degradation by batch air oxidation achieving simultaneously AC regeneration.

A small fixed bed reactor, 10 mm diameter, 0.18 m long, filled with granular activated carbon and equipped with convenient 3 way valves, may achieve successively the two main steps. Several AD-OX cycles have been performed with a phenol solution to quantify the regeneration of the activated carbon adsorption capacity. Results show that activated carbon is fast damaged during the first cycles, due to oxidative coupling, but then a quasi steady state is obtained proving that significant oxidative regeneration has been achieved.

A dynamic model of the adsorption step has been first developed, including intraparticle diffusion, liquid-solid external mass transfer and axial dispersion of the liquid phase. It has been applied to simulate the performance of the regenerated activated carbon.

Using oxidation kinetics over this aged carbon and its adsorption isotherm, separately determined in autoclave at reaction temperature, the oxidation step after several cycles has been simulated including the heating period, where desorption and oxidation simultaneously occur. The proposed model conveniently predicts the complex phenol concentration-time profile and gives insight to the hydrodynamic behavior of the recycle reactor and the role of mass transfer resistances.

Keywords

Water treatment, adsorption, activated carbon, oxidation, regeneration, three phase catalytic reactor, dynamics, hybrid process.

* *Corresponding author: Phone: +33 (0)5 34 32 37 09, Fax: +33 (0)5 34 32 37 00, Email: carine.julcour@ensiacet.fr*

† *Deceased on 1st June 2009*

1. Introduction

Wastewater treatment is of growing importance for sustainable development. Cheap and reliable processes should be developed to match the increasingly severe specifications on both toxic organic compounds and global chemical oxygen demand (COD).

One of the major techniques for the treatment of low concentrations of toxic organics in water is based on adsorption by Activated Carbon (AC), either in powdered or, most often, in granular form. AC adsorption can fully replace biological treatment, but it can be better used for eliminating biorefractory organics from water leaving conventional biological waste water treatment plants. AC adsorption as end step appears as the best technology according to Sarp Industries-Veolia[1].

Nevertheless this powerful technique, with regards to organic pollutant separation, highly suffers from economy and sustainability aspects, as the saturated activated carbon is either hardly regenerated – by non-environmental friendly ex situ high temperature processes – or even, for hazardous industrial wastewater, it becomes itself a solid waste to be incinerated. In situ regeneration would then be highly valuable.

Over the years a variety of regeneration techniques have been suggested, evaluated and applied. These methods are based either on desorption, induced by increasing temperature or by displacement with a solvent, or on chemical decomposition of the adsorbed species induced by thermal, chemical, electrochemical or microbial processes, as presented on Figure 1 according to Sheintuch and Matatov-Meytal[2].

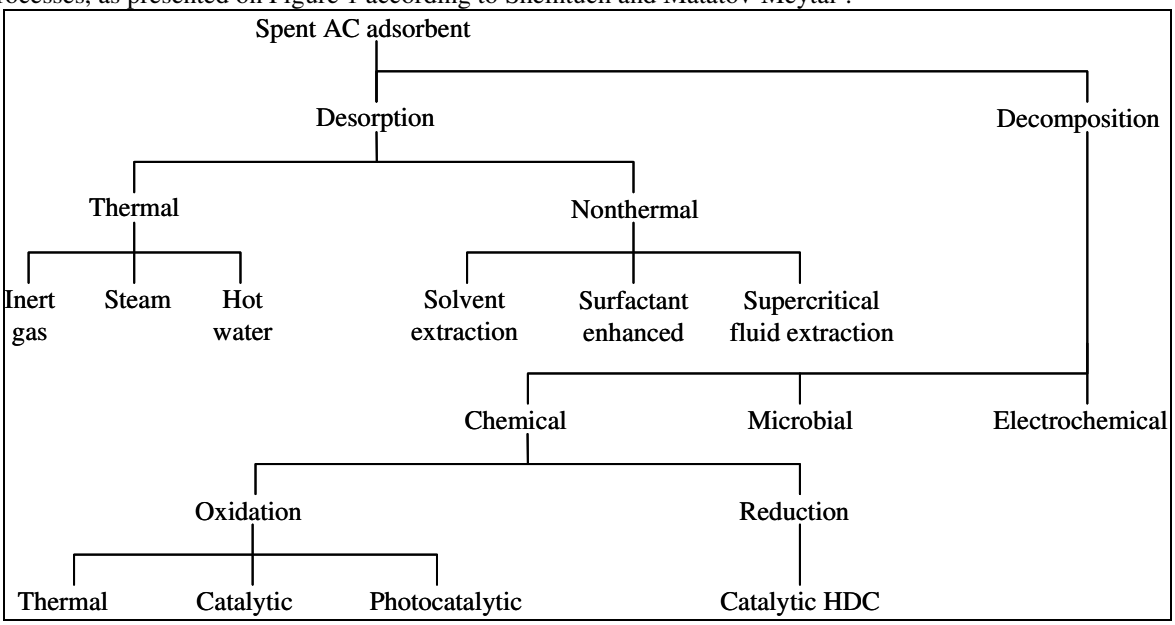

Figure 1. Overview of available techniques for regeneration of spent AC adsorbents (from Sheintuch and Matatov-Meytal, 1999)[2].

The most commonly used regeneration, thermal regeneration, based on either desorption with inert gas or reactive decomposition by water vapor or flue gas, needs very high temperature (700-1000°C) and then should only be achieved in few very large specialized units. It is not acceptable for hazardous compounds treated in industrial wastewater treatments.

Extractive regeneration methods that use volatile solvents (solvent regeneration) have been investigated, but current applications of this technology with AC are not known. Ethanol regeneration has been proposed but in any case a subsequent separation is still needed to recover the solvent. Supercritical fluid extraction exhibits enhanced mass-transfer properties over liquid solvent extraction. However, complete regeneration of AC loaded with organics like aromatic compounds could not be achieved using supercritical fluid extraction with CO_2 and a large amount of CO_2 would be required. As main drawback, such solvent regeneration serves only to transfer the contaminant from one location (AC) to another (solvent or surfactant) and does not destroy the pollutants which have to be treated subsequently.

Reactive regeneration methods appear much more attractive as they destroy the adsorbed organics by chemical processes (including acid–base or oxidative transformations, microbial or electrochemical processes). The chemical methods may involve complete mineralization of the adsorbed species (to carbon dioxide and water), transformation of complex molecules into simpler compounds and the conversion of hazardous materials to better desorbed, water-soluble or more biodegradable compounds. Chemical oxidation using various oxidants - chlorine, chlorine dioxide, hydrogen peroxide, Fenton's reagent, ozone and potassium permanganate - has been

tested[3-9] and at least partial restoration of AC adsorption capacity was demonstrated. Similarly unconventional techniques including electrochemistry[10-13], ultrasound[14], microwaves[15], electrodialysis[16] and plasma discharges[17] have been tried.
These advanced oxidation processes, however, have proven neither to be technically feasible for large scale continuous operation, nor to be economically viable.
An established technology for regeneration of spent AC with organics or oxidizable inorganic compounds is wet air regeneration (WAO), but this method is rather expensive because of the required large investments in high pressure equipment (~ 200 bar) and the high cost of running the regeneration at high pressure and temperature[18-19].
Catalytic regeneration methods may enhance the decomposition rates and enable to carry out the regeneration at lower temperatures and lower residence times. They could use either desorption followed by catalytic liquid-phase oxidation, or direct oxidation of the adsorbed species on an AC-adsorbent modified with a catalyst. In the former approach, the water is not contacted with the catalyst and metal dissolution is not a problem. In the latter approach, metal dissolution may occur and should be controlled.
The great improvement of the AD-OX process[20-21] is to achieve direct oxidation only with activated carbon which in this case catalyzes its own regeneration as adsorbent. The AD-OX process was first described and assessed for phenol/4-hydroxybenzoic acid mixture in a large reactor used for preliminary scale up[20]. In order to reduce the adsorption time for many successive runs, a small automated reactor was built up and tested with various effluents and activated carbons: examples are reported by Krou[22] for phenol and tartrazine solutions, as well as real effluent issued from biological treatment of industrial wastewater up to 20 cycles, and Julcour Lebigue *et al.*[21] using commercial AC and carbonaceous materials issued from sewage sludge.
Similar general trends were observed with all these systems. The present article focuses on data obtained with a commercial AC and a model phenol solution, yet better known concerning both adsorption and oxidation kinetics, and their analysis by detailed modeling of the two steps.

2. Experimental: procedures, investigated system and performance of the process

2.1. Experimental procedure

The successive adsorption-oxidation cycles were performed using a small fixed bed automated reactor (18 cm high and 1 cm internal diameter) to reduce the time required for bed saturation and investigate adsorbent ageing over many cycles. The schematic diagram of the set-up has been shown elsewhere[21].
It can switch from continuous adsorption which produces the purified water to batch oxidation at higher temperature and pressure which achieves catalytic adsorbent regeneration by means of three-way valves controlled by on-line analyzers: UV absorbance of the exit liquid stream during adsorption, and CO_2 concentration at the gas outlet during oxidation.
During the adsorption step, the fixed bed of activated carbon was continuously fed with the polluted solution (0.23 $L.h^{-1}$) until complete bed saturation - even the proposed process should stop at a maximum allowable outlet concentration. With successive bed saturations a better estimation of the variation of adsorption capacity of fresh/regenerated carbon may be achieved from numerical integration of the breakthrough curves.
After complete breakthrough was achieved, the batch oxidation step was started, the liquid being recycled through a loop including a pressurized tank filled with 400 mL of the phenol solution. The liquid recycling flow rate was set at 2.44 $L.h^{-1}$. The reactor was pressurized to 50 bar with air flowing cocurrently upward (30 NL/h). Simultaneously temperature was raised by heating the thermofluid circulating in the reactor jacket and in the gas-liquid preheater to the required oxidation temperature (typically 150°C).
After the oxidative regeneration of the adsorbent, the temperature of the reactor was decreased from 150°C to ambient, while maintaining gas and liquid circulation. Then the gas supply and liquid recycling were stopped, the pressure was released, and the valves switched to feed the reactor with fresh phenol solution so that another adsorption cycle could start.

2.2. Analytical methods

In addition to on-line analysis, liquid samples were taken periodically at the reactor outlet and in the pressurized tank and analyzed using HPLC with UV detection (UV6000 diode array detector, THERMO FINNIGAN). The separation was achieved using a C18 reverse phase column (ProntoSIL C18 AQ) with an isocratic mobile phase (40/60 mixture of acetonitrile and deionized water at pH 2.2) fed at 1 $mL.min^{-1}$. The wavelength was set to 254 nm for aromatic compound detection. Quantification was made from a calibration curve regularly updated with fresh standard solutions.

During oxidation the remaining chemical oxygen demand (COD) was also measured according to the closed-type reflux colorimetric method using potassium dichromate as oxidant (method for 0-150 and 0-1500 $mg.L^{-1}$ ranges[23]). Precision of the method had been assessed with standard solutions and showed a standard deviation of less than 5%.

2.3. Investigated system

As mentioned above, the AD-OX process was assessed with various effluents and activated carbons, and even in two reactors of different scales[20-22]. In order to achieve a complete model of the two steps, adsorption and oxidative regeneration in batch loop, a commercial AC and a phenol solution (5.3 $mol.m^{-3}$) have been selected as the model system to be investigated in the small scale reactor to faster carry out consecutive AD-OX cycles.
The commercial activated carbon (PICA F22, physico-chemical properties given in Table 1), was selected based both on its adsorption capacity for phenol, catalytic activity in CWAO and relative stability upon recycling measured in batch autoclave[24-25].
Five successive adsorption-oxidation cycles were performed on the small fixed bed set-up using 7.23 g of this AC (0.8 – 1 mm sieved fraction).

BET surface area ($m^2.g^{-1}$)	Microporous volume ($cm^3.g^{-1}$)	Mesoporous volume ($cm^3.g^{-1}$)	Oxygen content (%)	Ratio of acid to basic surface groups (-)	Ash content (%)	Iron content (ppm)
985	0.41	0.11	1.1	0.47	12	578

Table 1. Physico-chemical properties of the fresh activated carbon (PICA F22).

2.4. Performance of the AD-OX process

Figure 2 below shows the consecutive breakthrough curves of phenol obtained during the adsorption steps of five AD-OX cycles in the same conditions of concentration, flow rate and temperature..
During the first one, the adsorption front is rather steep and equilibrium is nearly achieved when the outlet concentration reaches 98% of the feed concentration: the amounts of adsorbed phenol, calculated from numerical integration of the breakthrough curve and from the corresponding isotherm, are very close: 1.9 $mol.kg^{-1}$ and 2 $mol.kg^{-1}$ respectively. So despite short contacting time, significant information on the adsorption behavior can be derived from this small scale reactor.
The main feature is the dramatic decrease of the adsorption capacity after the first oxidation, but then a quasi steady state is obtained to about one fifth of the original capacity. In other words the oxidative regeneration allows the carbon to treat twice its adsorption capacity over five cycles.
The loss of adsorption capacity can be related to the decrease of the carbon surface area and microporous volume (by about 50%). It has been already reported during the oxidation of phenols and usually attributed to the deposition of condensation products, irreversibly adsorbed and minimally oxidized, which block the access to micropores[26].

3. Modeling of the two steps

3.1. Adsorption step

3.1.1. Description of the model

The breakthrough curves were simulated by a model including liquid axial dispersion through series of stirred tanks, liquid-solid mass transfer, local adsorption equilibrium - assuming fast intrinsic adsorption kinetics and using Langmuir isotherm - and intraparticle diffusion according to the pore diffusion model. That means that an equivalent uniform diffusivity was calculated that in fact accounts for both surface and pore diffusion. Details of equations and numerical methods are given in Delmas *et al.*[20].

3.1.2. Model parameters

AC properties. As abovementioned, porosity and apparent density of the carbon varied during the AD-OX cycles: $\varepsilon_p = 0.52$ - $\rho_p = 993\ kg.m^{-3}$ for fresh AC, and $\varepsilon_p = 0.29$ - $\rho_p = 1459\ kg.m^{-3}$ for spent AC at the end of the five AD-OX series.

Adsorption isotherms. The adsorption isotherm of phenol was measured at 25°C on *fresh carbon*[21] and represented by a Langmuir isotherm on the concentration range of interest 0 – 5 $mol.m^{-3}$. The following values of q_{max} and K were obtained: $q_{max} = 2.11\ mol.kg^{-1}$ and $K = 4.08\ m^3.mol^{-1}$.

For *spent carbon*, the small amount of available material prevents from performing numerous adsorption tests which were carried out at 150°C only (as required for modeling the oxidation step). Preliminary tests proved the individual adsorption parameters to be less sensitive than diffusivity. Following the conclusions of a previous study[27], temperature was supposed to mainly affect the adsorption constant rather than the saturation capacity in the investigated range. Thus the saturation capacity at room temperature was set to the value measured at 150°C: q_{max} = 0.921 mol.kg^{-1} (cf. § 3.2.2). Then only the adsorption constant at 25°C had to be optimized together with the effective diffusivity thanks to a Gauss Newton technique by matching the exit concentration profiles.

3.1.3. Simulation results

As shown in Figure 2, both initial and last breakthrough curves are adequately fitted by the model.

Breakthrough curve on fresh AC. Optimization of effective diffusivity led to the following value: $D_{e,Ph}$ = $3.47 \cdot 10^{-9}$ m^2.s^{-1}, which is even higher than the molecular diffusivity of phenol ($D_{m,Ph} = 1.04 \cdot 10^{-9}$ m^2.s^{-1} according to Wilke and Chang equation). It can be thus concluded that surface diffusion is the predominant mechanism in the case of fresh F22 carbon, with porous diffusivity accounting only for 3 to 8% of effective diffusivity (according to the usual range of tortuosity factor).

Breakthrough curve on spent AC (last cycle). As expected fitting of the last breakthrough curve resulted in much lower values for both diffusivity and adsorption constant with respect to the fresh carbon, respectively $D_{e,Ph} = 3.55 \cdot 10^{-10}$ m^2.s^{-1} and K(25°C) = 0.086 m^3.mol^{-1}. Contribution of surface diffusion thus dropped for the spent carbon which pores are partly coated with organic condensation products.

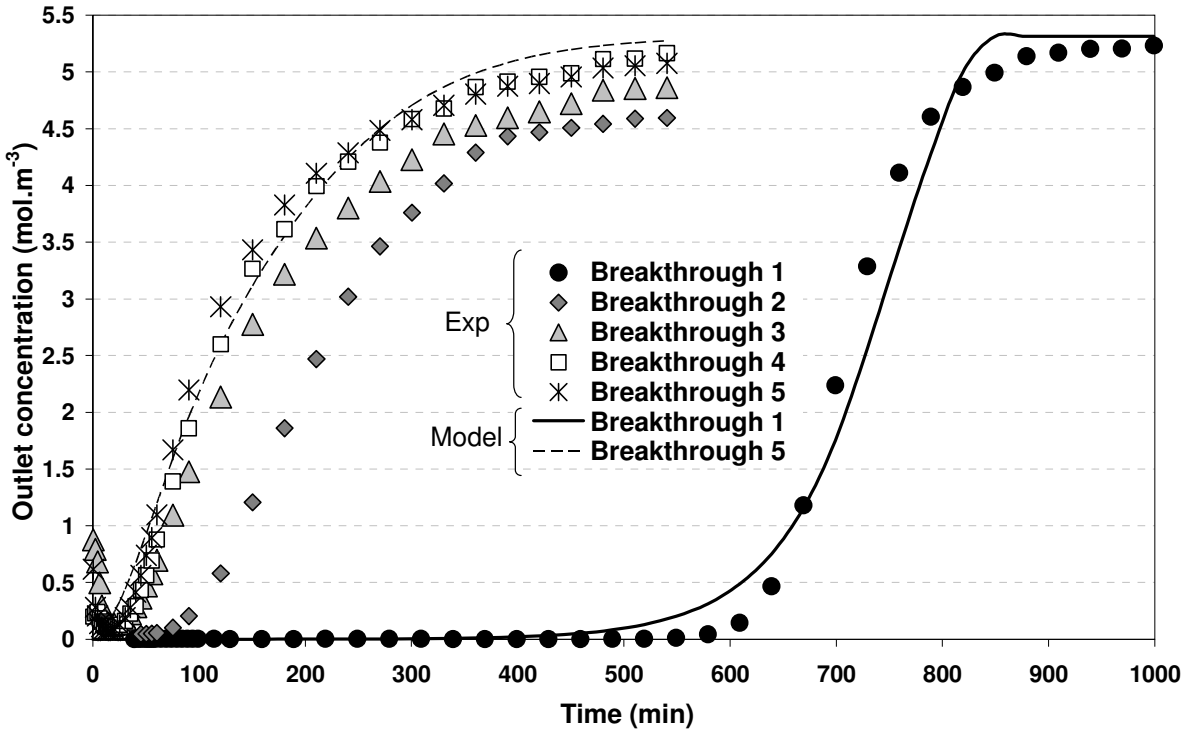

Figure 2. Successive breakthrough curves on PICA F22 (phenol adsorption) -
Q_L = 0.23 L.h^{-1} - C_{feed} = 5.3 mol.m^{-3} - m_{AC} = 7.23 g - T = 298.15 K: experimental and simulated profiles.

3.2. Oxidation step

The modeling of this step is more complex as phenol concentration varies due to two main reasons: oxidation and desorption. As shown in Figure 3a, the system consists in a fixed bed reactor (with axial gradients due to consumption of both phenol and oxygen), a liquid recycle loop and an intermediated tank (assumed perfectly mixed). Modeling of oxidation step was performed on the last cycle for which AC properties could be considered as stabilized and have been measured.

3.2.1. Description of the model

The following phenomena were accounted for:

- evolution of temperature and then of thermodynamics and kinetics, as oxygen was introduced during the heating period,

- diffusion of reactants (pollutant and oxygen) inside the AC pores,
- local adsorption/desorption equilibrium of the pollutant (described by Langmuir model),
- catalytic oxidation with full mineralization of the pollutant:

$$C_6H_6O\,(A) + 7O_2(B) \rightarrow 6CO_2 + 3H_2O$$

This assumption is supported by rather similar phenol and COD conversions showing that most of the phenol was oxidized to carbon dioxide and water[21].
The other *hypotheses* were:

- spherical and isothermal catalytic pellet,
- negligible temperature gradients, as gas and liquid were preheated and the exothermicity is low for the diluted reactant,
- insulated recycle loop,
- complete catalyst wetting, as the FBR operated in the upflow mode of gas-liquid flow,
- plug flow for gas phase, but axial dispersion effects accounted for liquid phase,
- negligible volume of connection tubes (no delay either between reactor outlet and tank inlet, or between tank outlet and reactor inlet),
- no solvent stripping (efficient condenser).

Model variables thus depend on time and up to two spatial coordinates, inside the reactor and inside the AC pellet and mass balances are described by the following equations:

Fixed bed reactor:

Liquid phase (plug flow with axial dispersion)

$$\frac{\partial(\varepsilon_{Lext}\cdot C_{LA})}{\partial t} = -\frac{\partial(u_{SL}\cdot C_{LA})}{\partial z} + \frac{\partial}{\partial z}\left(\varepsilon_{Lext}\cdot D_{axLA}\cdot\frac{\partial C_{LA}}{\partial z}\right) - (1-\varepsilon_B)\cdot\frac{3}{r_p}\cdot D_{e,A}(T)\cdot\left.\frac{\partial C_A}{\partial r}\right|_{r=rp} \quad (1)$$

$$\frac{\partial(\varepsilon_{Lext}\cdot C_{LB})}{\partial t} = -\frac{\partial(u_{SL}\cdot C_{LB})}{\partial z} + \frac{\partial}{\partial z}\left(\varepsilon_{Lext}\cdot D_{axLB}\cdot\frac{\partial C_{LB}}{\partial z}\right) + \left[k_La\cdot\left(C_{LB,sat} - C_{LB}\right)\right] - (1-\varepsilon_B)\cdot\frac{3}{r_p}\cdot D_{e,B}(T)\cdot\left.\frac{\partial C_B}{\partial r}\right|_{r=rp} \quad (2)$$

Gas phase (plug flow)

$$\frac{\partial(\varepsilon_{Gext}\cdot C_{GB})}{\partial t} = -\frac{\partial(u_{SG}\cdot C_{GB})}{\partial z} - k_La\cdot\left(C_{LB,sat} - C_{LB}\right) \quad (3)$$

(to account for oxygen consumption and resistance to gas-liquid mass transfer)

Catalytic phase

$$\varepsilon_p\cdot\frac{\partial C_B}{\partial t} = D_{e,B}(T)\cdot\left(\frac{1}{r^2}\cdot\frac{\partial}{\partial r}\left(r^2\cdot\frac{\partial C_B}{\partial r}\right)\right) - 7\cdot R_A \quad (4)$$

$$\varepsilon_p\cdot\frac{\partial C_A}{\partial t} + \rho_p\cdot\frac{\partial q_A}{\partial t} = D_{e,A}(T)\cdot\left(\frac{1}{r^2}\cdot\frac{\partial}{\partial r}\left(r^2\cdot\frac{\partial C_A}{\partial r}\right)\right) - R_A \text{ with } q_A = q_{max}\cdot\frac{K(T)\cdot C_A}{1+K(T)\cdot C_A} \quad (5)$$

Mixed tank: $$V_b\cdot\frac{dC_b}{dt} = Q_L\cdot\left((C_{LA})_{outlet} - C_b\right) \quad (6)$$

Boundary conditions:

Liquid phase:

$$z = 0, \quad \begin{cases} \dfrac{\varepsilon_{Lext}D_{axLA}}{u_{SL}}\dfrac{\partial C_{LA}}{\partial z} = (C_{LA})_{z=0} - C_b \\ \dfrac{\varepsilon_{Lext}D_{axLB}}{u_{SL}}\dfrac{\partial C_{LB}}{\partial z} = (C_{LB})_{z=0} - \left(C_{LB,sat}\right)_{inlet} \end{cases} \quad (7)$$

$$z = L_R, \quad \left(\frac{\partial C_{LA}}{\partial z}\right) = 0 \quad \text{et} \quad \left(\frac{\partial C_{LB}}{\partial z}\right) = 0 \quad (8)$$

Gas phase: $$z = 0, \quad C_{GB} = (C_{GB})_{inlet} = \frac{(P_{O2})_{inlet}}{RT} \tag{9}$$

Catalytic phase: $$r = 0, \quad \left(\frac{\partial C_A}{\partial r}\right) = 0 \quad \text{et} \quad \left(\frac{\partial C_B}{\partial r}\right) = 0 \tag{10}$$

$$r = r_p, \quad \begin{cases} -D_{e,A}(T)\frac{\partial C_A}{\partial r} = k_{LS,A}(C_A - C_{LA}) \\ -D_{e,B}(T)\frac{\partial C_B}{\partial r} = k_{LS,B}(C_B - C_{LB}) \end{cases} \tag{11}$$

Initial conditions: AC, the catalytic phase, is at adsorption equilibrium before starting the oxidation. The concentration of pollutant is uniform in the system, and the liquid phase is saturated with oxygen.
Thus for t = 0:

$$\forall r, \forall z \quad T = T_0$$
$$\forall r, \forall z \quad C_A = C_{LA} = C_b = C_0$$
$$\forall r, \forall z \quad q_A = q_{max}\frac{K(T_0)\cdot C_0}{1 + K(T_0)\cdot C_0}$$
$$\forall r, \forall z \quad C_B = C_{LB} = C_{LB,sat}(T_0)$$
$$\forall z \quad C_{GB} = C_{GB0} = \frac{(P_{O2})_0}{RT_0}$$

3.2.2. Model parameters

Oxidation kinetics. The intrinsic kinetics of phenol destruction was optimized from batch autoclave data using same pellets, catalytically stabilized after 3-4 adsorption/oxidation runs in similar operating conditions as in the FBR. A model accounting for transient diffusion of both oxygen and phenol inside the catalyst pores, lead to the following power law: $R_A = k_0 \cdot \exp\left(\frac{-E_a}{RT}\right) \cdot C_A^{\beta} \cdot x_B^{\alpha}$ (12)

with $\beta = 1$, $\alpha = 0.54$, $E_a = 6.46 \cdot 10^4$ J.mol^{-1} and $k_0 = 1.89 \cdot 10^8$ m^3.s^{-1}.m$^{-3}{}_{AC}$ [24-25].

Adsorption equilibrium. After the AD-OX runs, spent AC particles were washed with bidistilled water during a week so that to eliminate all reversibly-adsorbed components. After drying, phenol adsorption experiments were carried out on this aged AC loaded in a batch autoclave to get isotherm at 150°C. They were performed under low stirring (600 rpm) and under nitrogen pressure (12 bar) to prevent simultaneous oxidation. The corresponding isotherm was fitted by a Langmuir equation with the following parameters: q_{max}(150°C) = 0.921 mol.kg^{-1} and K(150 °C) = 0.027 m^3.mol^{-1}.

Using previous calculations on breakthrough curve (assuming a negligible effect of temperature on q_{max} value), the evolution of the adsorption constant of the spent AC as a function of temperature could be deduced from[28]:

$$K = K_{\infty} \cdot \exp\left(\frac{Q_{ads}}{R \cdot T}\right) \tag{13}$$

with $K_{\infty} = 1.60 \cdot 10^{-3}$ m^3.mol^{-1}, $Q_{ads} = 9.92$ kJ.mol^{-1}.

Hydrodynamics and mass transfer. Table 2 lists both the literature correlations selected and the corresponding set of values of key model parameters.

Parameter	Correlation	Value
ε_{Lext}	Yang *et al.*[29]	0.43
D_{axLA} (m^2.s^{-1})	Stüber[30] based on Syaiful[31]	$4.22 \cdot 10^{-5}$
D_{axLB} (m^2.s^{-1})	Stüber[30] based on Syaiful[31]	$4.22 \cdot 10^{-5}$
$k_{LS,A}$ (m.s^{-1})	Specchia *et al.*[32]	$7.61 \cdot 10^{-4}$
$k_{LS,B}$ (m.s^{-1})	Specchia *et al.*[32]	$1.83 \cdot 10^{-3}$
k_La (s^{-1})	Saada[33]	0.77

Table 2. Hydrodynamic and mass transfer parameters for reference case (T=423.15 K - P = 50 bar - Q_L = 2.44 L.h^{-1} - Q_{air} = 30 NL.h^{-1}).

Dynamic temperature profile. The experimental time temperature profile measured at the bed outlet during the heating period was conveniently represented by a rational function fitting as shown on Figure 3b.

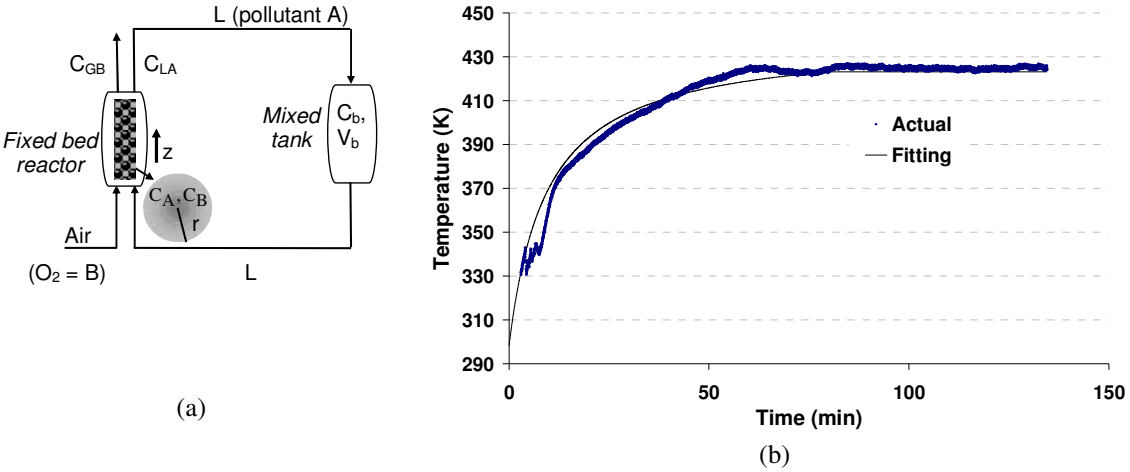

Figure 3. (a) Simplified scheme of AD-OX set-up, (b) fitting of experimental outlet temperature during heating period.

3.2.3. Numerical solution

COMSOL Multiphysics software was used to solve the set of partial differential equations, coupling macro- and microscale phenomena.

This software uses finite element method for spatial resolution and backward differentiation formula method for time integration.

The simulation strategy consisted in expressing the above equations in terms of dimensionless variables x (= z/L_R) and y (= r/r_p) and representing the catalyst particles according to a 2D geometry using these two independent variables[34]: diffusion-reaction equations were only solved along y variable giving the source term of equations (1) and (2), while x variable allowed to set the actual boundary condition on the pellet surface according to its position along the packed bed (calculated by the 1D fixed bed model).

3.2.4. Preliminary simulations

To assess the model and better understand the limiting phenomena, a first simulation was performed setting the system temperature to a constant value of 150°C, just as if heating was instantaneous.

For consistency, a pseudo-initial concentration of phenol in the liquid phase was calculated from a simple balance on the whole system assuming adsorption equilibrium shifted from 25°C to 150°C.

In Figure 4, this simulation is compared to the experimental time concentration profile inside the tank when starting from 25°C.

The model predicts a quasi-exponential decay of concentration due to an almost linear portion of the spent AC isotherm in the investigated range of concentrations. Conversely, the experimental phenol concentration versus time plot exhibits a clear peak, due to the desorption of the pollutant when increasing the temperature (from 25°C to 150°C) which first dominates due to negligible reaction rates under 100°C. As expected, the predicted decrease is thus faster than the experimental data as the initial heating period of about one hour is not accounted for. Nevertheless the simulation matches actual data at the end.

The model prediction is also compared to that of a much simpler one, describing the FBR as a perfectly mixed tank with liquid phase saturated by oxygen. They actually match as both phenol and oxygen concentrations in the liquid phase exhibit flat axial profiles due to the high recycle flow and oxygen excess (cf. Figure 5). k_La coefficient supplied by the correlation also results in an efficient transfer as the concentration of oxygen in the liquid phase differs by 8% at most from the saturation value.

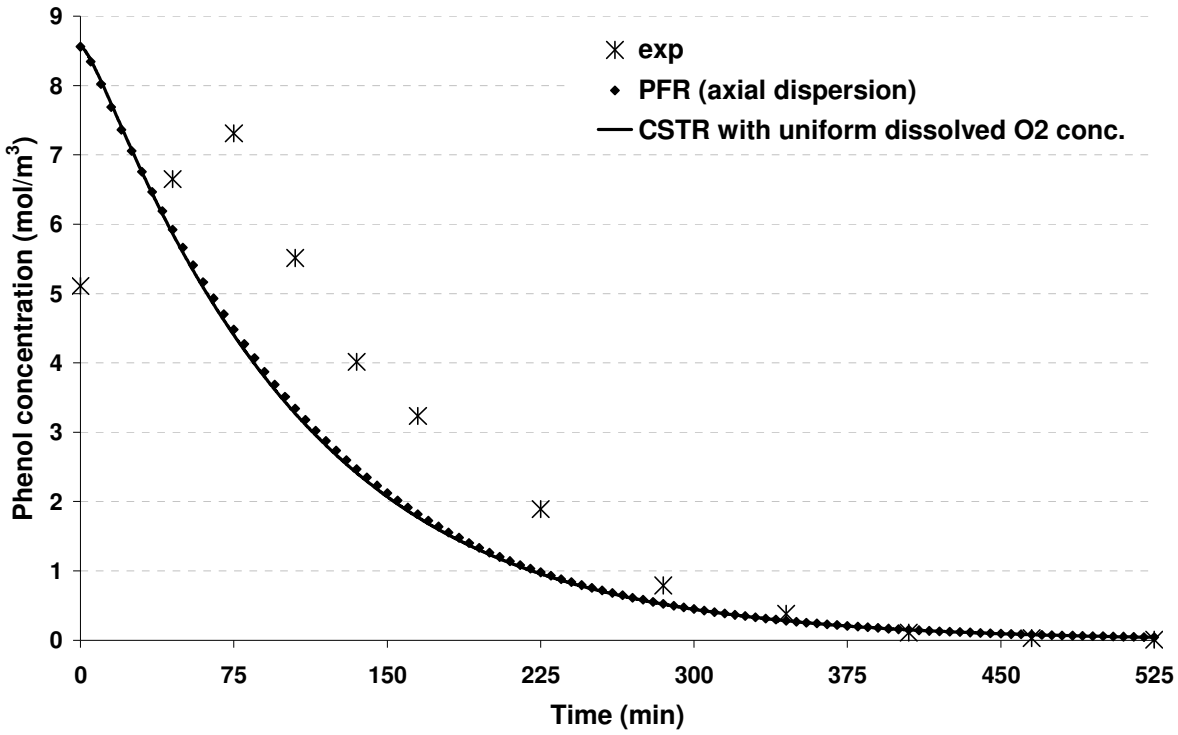

Figure 4. Evolution of phenol concentration in the mixed tank during last oxidation step – w_{AC} = 7.23 g - Q_L = 2.44 L.h^{-1} - Q_{air} = 30 NL.h^{-1} - P = 50 bar - T = 423.15 K: experimental and simulated profiles.*

*(*assuming constant temperature)*

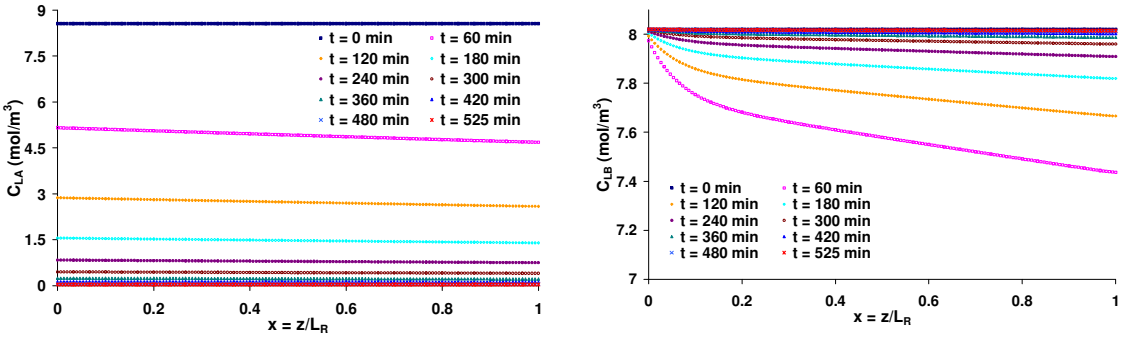

(a) (b)

Figure 5: Axial concentration profiles of phenol (a) and oxygen (b) in the FBR (assuming constant temperature) – w_{AC} = 7.23 g - Q_L = 2.44 L.h^{-1} - Q_{air} = 30 NL.h^{-1} - P = 50 bar - T = 423.15 K.

3.2.5. Simulation including heating period under air

Figures 6 and 7 show the results of the model when accounting for the evolution of the system temperature during the heating period, according to Figure 3b.

Same trend is now obtained for both experimental and simulation curves in Figure 6, except some shift of maxima, which could be due to either slow desorption dynamics or the existence of temperature gradients along the FBR due to poor heat transfer from the jacket to the fixed bed and defective loop insulation.

The concentration of oxygen at the pellet surface decreases regularly due to the decrease of solubility with temperature and the radial profile deepens only when temperature is high enough to observe diffusion limited reaction (above 100°C) (Figure 7a). On the contrary, phenol concentration (Figure 7b) first increases and early exhibits an inversed profile with a maximum at the pellet center due to desorption. Then, when sufficient temperature is achieved for oxidation to prevail, the two profiles deepen due to limiting diffusion. As expected, the concentration gradients are then much more pronounced for oxygen (limiting reactant) than for phenol.

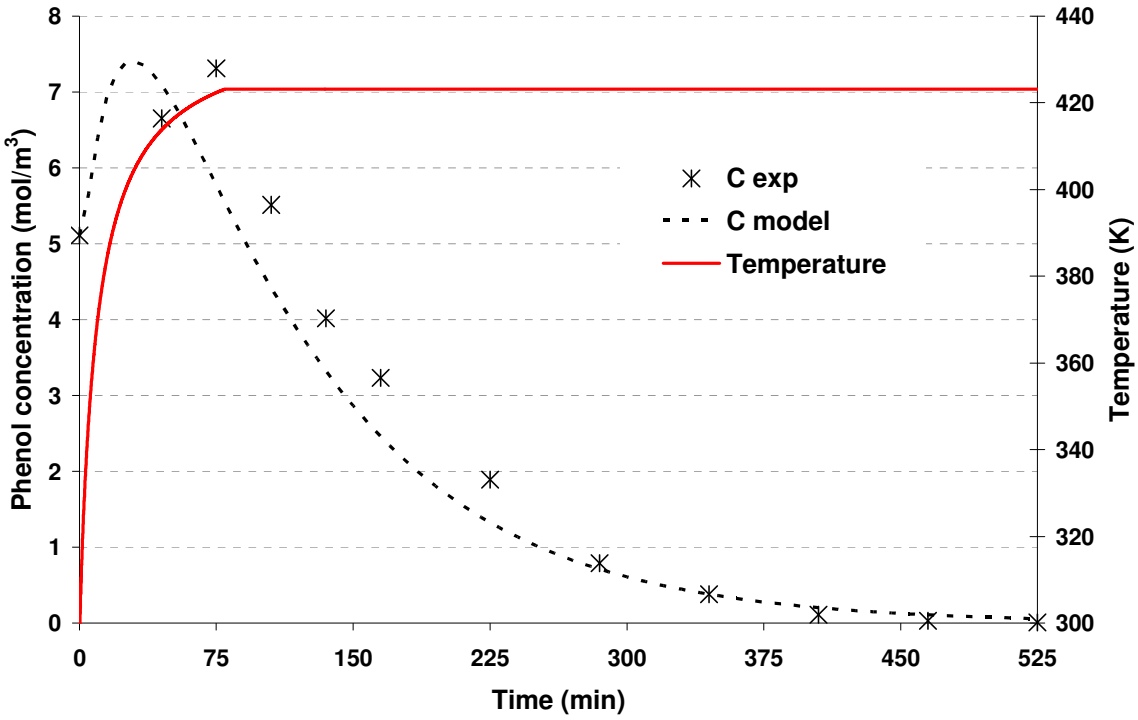

Figure 6. Evolution of temperature and phenol concentration in the mixed tank during last oxidation step – w_{AC} = 7.23 g - Q_L = 2.44 L.h^{-1} - Q_{air} = 30 NL.h^{-1} - C_0 = 5.3 mol.m^{-3} - P = 50 bar - T = 423.15 K: experimental and simulated profiles.

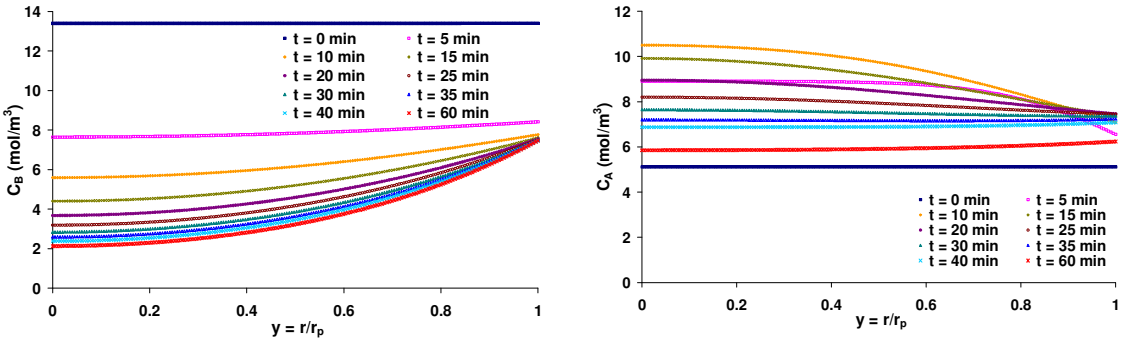

(a) (b)

Figure 7. Radial concentration profiles of oxygen (a) and phenol (b) in the AC pellet – w_{AC} = 7.23 g - Q_L = 2.44 L.h^{-1} - Q_{air} = 30 NL.h^{-1} - C_0 = 5.3 mol.m^{-3} - P = 50 bar - T = 423.15 K.

4. Conclusion

The sequential adsorption-oxidation process (AD-OX) was investigated in an automated small-size multifunctional reactor with a commercial activated carbon. After being validated as a post-biological treatment of industrial wastewater over 20 cycles, it was more carefully investigated using model phenol solution.

A complete simulation of the two successive steps has been performed. The dramatic decrease in adsorption efficiency of the aged AC is due to formation of heavy condensation compounds, involving a reduction of the microporous volume. In addition breakthrough simulation suggests a strong decrease of surface diffusivity.

The most original contribution of this work is the simulation of the oxidation step in the batch loop including the three-phase catalytic reactor. It involves simultaneous desorption and oxidation during the heating period, using

high temperature adsorption isotherm and oxidation kinetics obtained separately. The main trends are conveniently predicted without any fitting parameter: first fast desorption, then prevailing oxidation at higher temperature. Mass transfer limitations are clearly shown, especially oxygen diffusion, and unusual information on the evolution of oxygen and phenol concentration profiles in AC particles is also provided.

AD-OX as a potential post-treatment of industrial wastewater suffers from the dramatic reduction of AC adsorption capacity (about 80%) at the very first oxidation. Nevertheless the AC is then fast stabilized (after 2-3 cycles), opening the way to a possible sustainable process. The future of such process would depend on the number of possible recycles with similar performances, which of course should be much higher than five as tested in this work. In addition better regeneration conditions (lower temperature) could be achieved with doped activated carbon - e.g. Fe/AC catalyst - in order to preserve adsorption capacity preventing severe oxidative coupling. Finally with the best oxidative conditions, the regeneration duration should also be optimized through cost calculation.

Notations

C	Concentration ($mol.m^{-3}$)
C_b	Concentration of phenol in the mixed tank ($mol.m^{-3}$)
D_{ax}	Axial dispersion coefficient ($m^2.s^{-1}$)
d_p	Particle diameter (m)
D_e	Effective diffusivity ($m^2.s^{-1}$)
D_m	Molecular diffusivity ($m^2.s^{-1}$)
K	Langmuir adsorption constant ($m^3.mol^{-1}$)
k_La	Gas – liquid volumetric mass transfer coefficient (s^{-1})
k_{LS}	Liquid – solid mass transfer coefficient ($m.s^{-1}$)
P	Total pressure (bar)
P_{O2}	Oxygen partial pressure (Pa)
Q	Volumetric flow rate ($m^3.s^{-1}$ or $L.h^{-1}$)
Q_{ads}	Adsorption heat ($J.mol^{-1}$)
q_{max}	Langmuir saturation capacity ($mol.kg^{-1}$)
r	Particle radial dimension (m)
R	Universal gas constant ($J.mol^{-1}.K^{-1}$)
R_A	Phenol oxidation rate ($mol.m^{-3}.s^{-1}$)
r_p	Particle radius (m)
t	Time (s)
T	Temperature (K)
u_S	Superficial velocity ($m.s^{-1}$)
V_b	Volume of liquid in the mixed tank (m^3)
w_{AC}	Activated carbon weight (g)
x_B	Liquid molar fraction of reactant B (-)
z	Fixed bed axial dimension (m)
Greek symbols	
ε_B	Fixed bed void fraction (-)
ε_{Gext}	External gas hold-up (-)
ε_{Lext}	External liquid hold-up (-)
ε_p	Porosity of AC particle (-)
ρ_p	Apparent density of AC particle ($kg.m^{-3}$)
Subscripts	
0	Initial
A, B	Reactant A (phenol), Reactant B (oxygen)
G, L	Gas phase, Liquid phase

Acknowledgements

European Community through the 6th FP ("REMOVALS" STREP project) and Agence Nationale de la Recherche ("PHARE" Precodd project) are acknowledged for financial support.

The authors also thank L. Pollini, F. Dunglas, J.L. Nadalin, I. Coghe, L. Farhi (LGC) for technical assistance and PICA (VEOLIA group) for providing activated carbon.

References

[1] Sarp Industries - Veolia, private communication, **2009**.

[2] Sheintuch, M. and Matatov-Meytal, Y.I. Comparison of catalytic processes with other regeneration methods of activated carbon. *Catal. Today* **1999**, *53*, 73.

[3] Horng, R.S. and Tseng, I.C. Regeneration of granular activated carbon saturated with acetone and isopropyl alcohol via a recirculation process under H_2O_2/UV oxidation. *J. Hazard. Mater.* **2008**, *154*, 366.

[4] Liang, G.; Lin, Y.T.; Shin, W.H. Persulfate regeneration of trichloroethylene spent activated carbon. *J. Hazard. Mater.* **2009**, *168*, 187.

[5] Bento, L.R.S.M. and Rein, P.W. Chemical regeneration of activated carbon. *US Patent Application #: 20080286193WO/2007/032998, International Application No.: PCT/US2006/034925*, **2007**.

[6] Huling, S.G.; Jones, P.K.; Ela, W.P.; Arnold, R.G. Fenton-driven chemical regeneration of MTBE-spent GAC. *Water Res.* **2005**, *39*, 2145.

[7] Arnold, R.G. In-situ Regeneration of Granular Activated Carbon (GAC) Using Fenton's Reagents, **2006**. http://superfund.pharmacy.arizona.edu/research%20translation/Regeneration_GAC_using_FentonsFinal%20Report%2706.pdf

[8] Toledo, L.C.; Silva, A.C.B.; Augusti, R.; Lago, R.M. Application of Fenton's reagent to regenerate activated carbon saturated with organochloro compounds. *Chemosphere* **2003**, *50*, 1049.

[9] Alvarez, P.; Garcia-Araya, J.; Beltran, F.; Masa, F.; Medina, F. Ozonation of activated carbons: Effect on the adsorption of selected phenolic compounds from aqueous solutions. *J. Colloid Interf. Sci.* **2005**, *283*, 503.

[10] Weng, C.H. and Hsu, M.C. Regeneration of granular activated carbon by an electrochemical process. *Sep. Purif. Technol.* **2008**, *64 (2)*, 227.

[11] Zhang, H. Regeneration of exhausted activated carbon by electrochemical method. *Chem. Eng. J.* **2002**, *85 (1)*, 81.

[12] Zhou, M.H. and Lei, L.C. Electrochemical regeneration of activated carbon loaded with p-nitrophenol in a fluidized electrochemical reactor. *Electrochim. Acta* **2006**, *51 (21)*, 4489.

[13] Narbaitz, R.M. and Karimi-Jashni, A. Electrochemical regeneration of granular activated carbons loaded with phenol and natural organic matter. *Environ. Technol.* **2009**, *30 (1)*, 27.

[14] Saoudi, F.; Hamdaoui, O. Innovative technique for 4-chlorophenol desorption from granular activated carbon by low frequency ultrasound: Influence of operational parameters. *Microporous Mesoporous Mater.* **2011**, *141*, 69.

[15] Ania, C.O.; Parra, J.B.; Menéndez, J.A.; Pis, J.J. Effect of microwave and conventional regeneration on the microporous and mesoporous network and on the adsorptive capacity of activated carbons. *Microporous Mesoporous Mater.* **2005**, *85 (1-2)*, 7.

[16] Drouiche, N.; Mahmoudi, M.; Mameri, N.; Lounici, H.; Ghaffour, N. Utilization of electrodialysis for the regeneration of granular activated carbon packed in beds saturated with H_2S. *Desalination* **2006**, *200 (1-3)*, 629.

[17] Qu, G.Z.; Li, J.; Wu, Y.; Li, G.F.; Li, D. Regeneration of acid orange 7-exhausted granular activated carbon with dielectric barrier discharge plasma. *Chem. Eng. J.* **2009**, *146*, 168.

[18] Gonzalez, J.F.; Encinar, J.M.; Ramiro, A.; Sabio, E. Regeneration by Wet Oxidation of an Activated Carbon Saturated with p-Nitrophenol. *Ind. Eng. Chem. Res.* **2002**, *41 (5)*, 1344.

[19] Shende, R.V. and Mahajani, V.V. Wet oxidative regeneration of activated carbon loaded with reactive dye. *Waste Manage.* **2002**, *22*, 73.

[20] Delmas, H.; Creanga, C.; Julcour-Lebigue, C.; Wilhelm, A.M. AD-OX: A sequential oxidative process for water treatment- adsorption and batch CWAO regeneration of activated carbon. *Chem. Eng. J.* **2009**, *152 (1)*, 189.

[21] Julcour Lebigue, C.; Andriantsiferana, C.; Krou, N.; Ayral, C.; Mohamed, E.; Wilhelm, A.M.; Delmas, H.; Le Coq, L.; Gerente, C.; Smith, K.M.; Pullket, S.; Fowler, G.D.; Graham N.J.D. Application of sludge-based carbonaceous materials in a hybrid water treatment process based on adsorption and catalytic wet air oxidation. *J. Environ. Manage.* **2010**, *91*, 2432.

[22] Krou, N.J. Etude expérimentale et modélisation d'un procédé séquentiel AD-OX d'élimination de polluants organiques. *Ph. D. thesis INP Toulouse,* France **2010**. *ethesis.inp-toulouse.fr/archive/00001145/01/krou.pdf*

[23] Hach Company, DR/2500 Spectrophotometer Procedure Manual, Edition 4, Oxygen Demand, Chemical: Reactor Digestion Method, **2003**.

[24] Ayral, C.; Julcour-Lebigue, C.; Stüber, F.; Wilhelm, A.M.; Delmas, H. Catalytic wet air oxidation of phenolic compounds and mixtures on activated carbons: conversion, mineralization and catalyst stability. *Ind. Eng. Chem. Res.* **2010**, *49*, 10707.

[25] Ayral, C. Elimination de polluants aromatiques par oxydation catalytique sur charbon actif. *Ph. D. thesis INP Toulouse*, France **2009**. *ethesis.inp-toulouse.fr/archive/00000931/01/ayral.pdf*

[26] Cordero, T.; Rodriguez-Mirasol, J.; Bedia, J.; Gomis, S.; Yustos, P.; Garcia-Ochoa, F.; Santos, A. Activated carbon as catalyst in wet oxidation of phenol: Effect of the oxidation reaction on the catalyst properties and stability. *Appl. Catal. B* **2008**, *81*, 122.
[27] Creanga Manole, C.; Julcour-Lebigue, C.; Wilhelm, A.M.; Delmas, H. Catalytic oxidation of 4-hydroxybenzoic acid on activated carbon in batch autoclave and fixed bed reactor. *Ind. Eng. Chem. Res.* **2007**, *46 (25)*, 8388.
[28] Do, D.D. Adsorption analysis: Equilibria and Kinetics, Series on Chemical Engineering, *Imperial College Press* (vol.2) **1998**.
[29] Yang, X.L.; Euzen, J.P.; Wild, G. Etude de la rétention liquide dans les réacteurs à lit fixe avec écoulement ascendant de gaz et de liquide. *Entropie* **1989**, *150*, 17.
[30] Stüber, F. Sélectivité en réacteur catalytique triphasique : analyse expérimentale et théorique d'hydrogénations consécutives en lit fixe catalytique à co-courant ascendant de gaz et de liquide. *Ph. D. thesis INP Toulouse, France* **1995**.
[31] Syaiful. Réacteurs polyphasiques à co-courant ascendant : influence de la viscosité sur les rétentions, dispersions axiales et transfert gaz – liquide. *Ph. D. thesis INP Toulouse, France* **1992**.
[32] Specchia, V.; Baldi, G.; Gianetto, A. Solid-liquid mass transfer in concurrent two-phase flow through packed beds. *Ind. Eng. Chem. Proc. Des. Dev.* **1978**, *17 (3)*, 362.
[33] Saada, M.Y. Assessment of interfacial area in co-current two-phase flow in packed beds. *Chim. Ind., Génie Chim.* **1972**, *105 (20)*, 1415.
[34] FEMLAB, example model solved with the chemical engineering module, packed bed reactor, COMSOL **2002**.